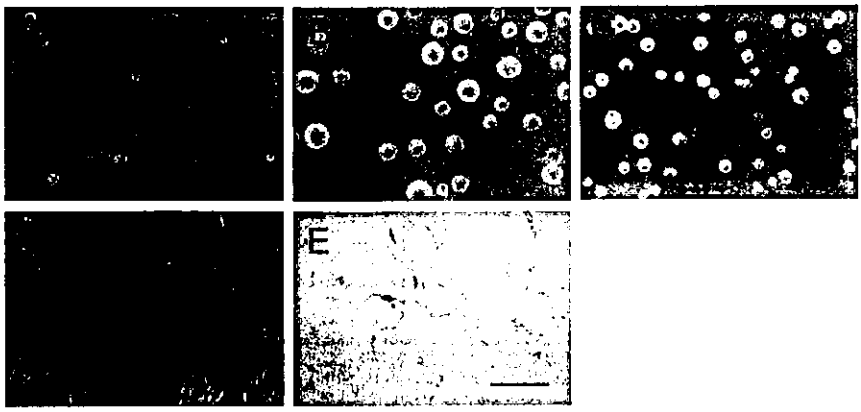

FIG. 1. Phase-contrast micrographs showing isolated germ cells and Sertoli cells from a testicular cell suspension. A) Type A spermatogonia. B) Spermatocytes. C) Spermatids. D) Sertoli cells. E) Alkaline phosphatase activity of Sertoli cell cultures. Germ cells in A–C were from testes of 8-wk-old mice. Sertoli cells in D and E were from testes of 2-wk-old mice. Scale bar = 30 μm.

from two 8-wk-old adult mice. The purity of each isolated population was <84.5% (Fig. 1A and Table 1). Using phase-contrast microscopy, we determined that these cells were 14–16 μm in diameter. Following elimination of the remaining spermatogonia using magnetic microbeads, the remaining cells were separated into two principal visible bands by centrifugation through a discontinuous Percoll gradient. Phase-contrast microscopy revealed that these two bands consisted primarily of pachytene spermatocytes and round spermatids (Fig. 1, B and C). We isolated an average of 3×10^5 spermatocytes and 200×10^5 spermatids from two 8-wk-old adult mice. We also isolated an average 20×10^5 Sertoli cells from ten 2-wk-old juvenile mice (Fig. 1D). Peritubular myoid cells were identified by alkaline phosphatase staining. Although >95% of these cells were unstained, ~5% of the Sertoli cells showed considerable alkaline phosphatase activity (Fig. 1E).

RT-PCR Analysis of Isolated Cells Expressing Specific Marker Genes

RT-PCR using extracts of isolated cells confirmed the expression of mRNAs from *c-kit*, Histone H1t, *SP-10*, and *SCF*. Each gene was expressed in only one cell type, as follows: *c-kit* in spermatogonia, the Histone H1t gene in spermatocytes, *SP-10* in spermatids, and *SCF* in Sertoli cells (Fig. 2).

Characterization of Isolated Cells by FACS

To determine the purity of isolated germ cells, we used FACS analysis to follow the differentiation-dependent acquisition of stage-specific patterns during spermatogenesis and monitored the percentage of cells with differing DNA content. The histogram in Figure 3 presents the number of cells at each fluorescence level (FL2-A). Diploid (2n DNA) cells were observed in 84.5% of the isolated spermatogonia, tetraploid (4n DNA) cells were observed in 79.6% of the isolated spermatocytes, and haploid (1n DNA) cells were observed in 85.3% of the isolated spermatids (Table 1). These results demonstrate that the majority of cells in each population exhibited the expected ploidy.

TABLE 1. The percentage of 1n, 2n, and 4n cells in isolated germ cells from a testicular cell suspension from 8-wk-old mice, as determined by FACS.[a]

Ploidy[b]	Total cells (%)[c]	Isolated germ cells (%)		
		Spermatogonia	Spermatocytes	Spermatids
1n	56.2 ± 4.2	9.4 ± 1.2	5.3 ± 1.8	85.3 ± 3.3
2n	25.2 ± 3.6	84.5 ± 2.7	9.3 ± 1.3	6.2 ± 0.9
4n	18.6 ± 3.1	12.7 ± 0.9	79.6 ± 2.5	7.7 ± 2.2

[a] Calculated after eliminating cell debris (FL2-A < 50 in Fig. 2).
[b] 1n, haploid cells (one copy of genome); 2n, diploid cells (two copies of genome); 4n, tetraploid cells (four copies of genome).
[c] Each percentage represents the mean ± SD of 4–6 measurements.

Expression of UCH Isozymes During Spermatogenesis

We characterized the expression pattern of each UCH gene in isolated testicular cell populations during spermatogenesis using SYBR Green-based real-time quantitative RT-PCR (Fig. 4). The 2^{-ddCt} values indicate the relative mRNA expression levels compared with spermatogonia from 2-wk-old mice (Sg2). The genes encoding UCH-L1 and UCH-L4 were expressed mainly in spermatogonia (Fig. 4, A and C). UCH-L1 was also expressed significantly in the Sertoli population, and UCH-L4 was expressed to a lesser degree in spermatocytes and spermatids. UCH-L3 and UCH-L5 genes were expressed primarily in the spermatid population and to a much lesser extent in spermatocytes (Fig. 4, B and D). We further examined the expression of UCH mRNAs during testicular maturation (Fig. 5A) in whole testes from 5-, 7-, 15-, 19-, 21-, 23-, 26-, and 33-

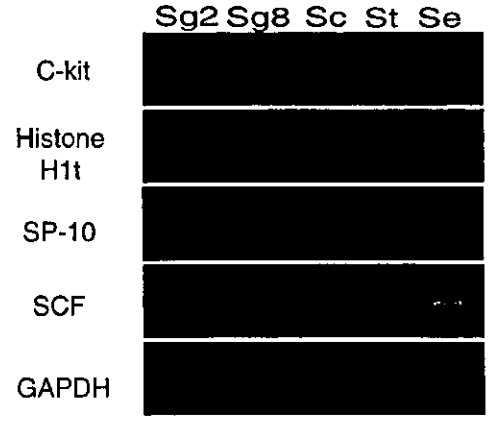

FIG. 2. Expression of c-kit, Histone H1t, SP-10, and SCF mRNAs determined by RT-PCR of extracts of isolated germ cells and Sertoli cells from a testicular cell suspension. Sg2, Spermatogonia of 2-wk-old mice; Sg8, spermatogonia from 8-wk-old mice; Sc, spermatocytes from 8-wk-old mice; St, spermatids from 8-wk-old mice; Se, Sertoli cells from 2-wk-old mice.

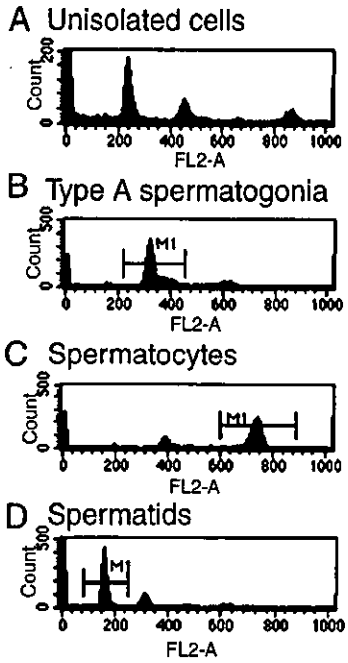

FIG. 3. FACS analysis of isolated germ cells from a testicular cell suspension obtained from 8-wk-old mice. Each window is a histogram representing the number of cells at each fluorescence level (FL2-A). A) Unisolated cells. B) Type A spermatogonia. C) Spermatocytes. D) Spermatids.

day-old mice. The UCH-L1 and UCH-L4 mRNAs were expressed similarly during development and likewise for the UCH-L3 and UCH-L5 genes. The expression of UCH-L1 mRNA appears relatively high on Postnatal Day 15. However, the percentage of spermatogonia and Sertoli cells would have become diluted by meiotic and postmeiotic germ cells after Day 15, thereby accounting for the relatively lower levels of UCH-L1 at subsequent time points. RT-PCR data suggest that UCH-L1 mRNA expression in spermatogonia and Sertoli cells increased continuously even after Postnatal Day 15 (Fig. 5B). We also analyzed the protein expression patterns of UCH-L1 and UCH-L3 in the mouse testis using peptide-specific antibodies that recognize regions in mouse UCH-L1 or UCH-L3. Western blot analysis detected UCH-L1 in spermatogonia and Sertoli cells, and UCH-L3 was detected primarily in spermatocytes and spermatids, as expected, although it was also found to a lesser extent in spermatogonia (Fig. 6A). Also, UCH-L3 expression increased in a differentiation-dependent manner during juvenile spermatogenesis (Fig. 5C). Immunohistochemistry detected homogeneous UCH-L1 expression in both spermatogonia and Sertoli cells from wild-type (Balb/c) and *Uchl3* knockout mice, whereas UCH-L3 was detected mainly in spermatocytes and round spermatids of wild-type (Balb/c) and *gad* mice (Fig. 6, B and C).

DISCUSSION

The ubiquitin pathway plays critical roles in the progression of spermatogenesis through the mitotic, meiotic, and postmeiotic phases [2, 3, 18, 36]. Because numerous proteins are regulated by ubiquitination, mutations that affect the ubiquitin pathway result in the dysregulation of multiple cellular processes and induce apoptosis during spermatogenesis [3, 37–39]. For example, mutation of HR6B, a ubiquitin-conjugating enzyme, affects both meiosis and postmeiotic germ cell development [40–43].

Ubiquitin C-terminal hydrolases catalyze the hydrolysis of C-terminal esters and amides of ubiquitin. These enzymes are believed to play a key role in processing polyubiquitin and ubiquitylated proteolytic peptides [8]. The genes for at least four UCHs, UCH-L1 and UCH-L3–5, have been identified in the mouse. Although the specificity and function of these isozymes in spermatogenesis remains elusive, each of these enzymes contains conserved residues that are critical for enzymatic activity [8–10, 44, 45]. The predominant mouse isozymes, UCH-L1 and UCH-L3, share 52% amino acid sequence identity [10, 13, 45]. However, UCH-L1 mRNA is selectively expressed in the mouse testis and nervous systems [11], whereas UCH-L3 mRNA is expressed in nearly every tissue tested, with high levels in the testis [13]. Intracellular localization of UCH-L1 was reported to be closely associated with the proliferative activity of spermatogonia and Sertoli cells [15–18]. In contrast, the expression of UCH-L3 has not been examined in the testis. To address this question, we first generated poly-

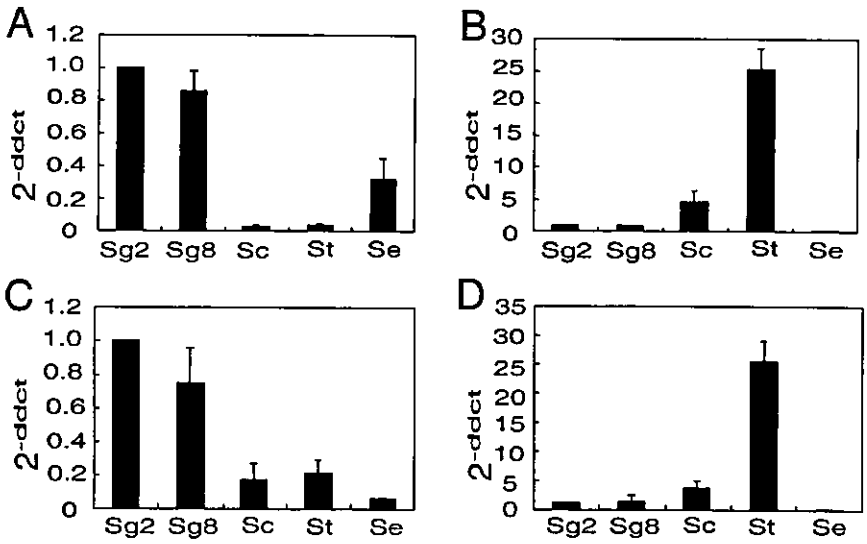

FIG. 4. Comparison of the relative UCH isozyme gene expression levels (2^{-ddCt}) in isolated germ cells and Sertoli cells using RT-PCR. The formula 2^{-ddCt} indicates the relative expression level in isolated testicular cells compared with Sg2 cells. Sg2 gene expression in each case was set to 1.0. A) *Uchl1*. B) *Uchl3*. C) *Uchl4*. D) *Uchl5*. Sg2, Spermatogonia from 2-wk-old mice; Sg8, spermatogonia from 8-wk-old mice; Sc, spermatocytes from 8-wk-old mice; St, spermatids from 8-wk-old mice; Se, Sertoli cells from 2-wk-old mice.

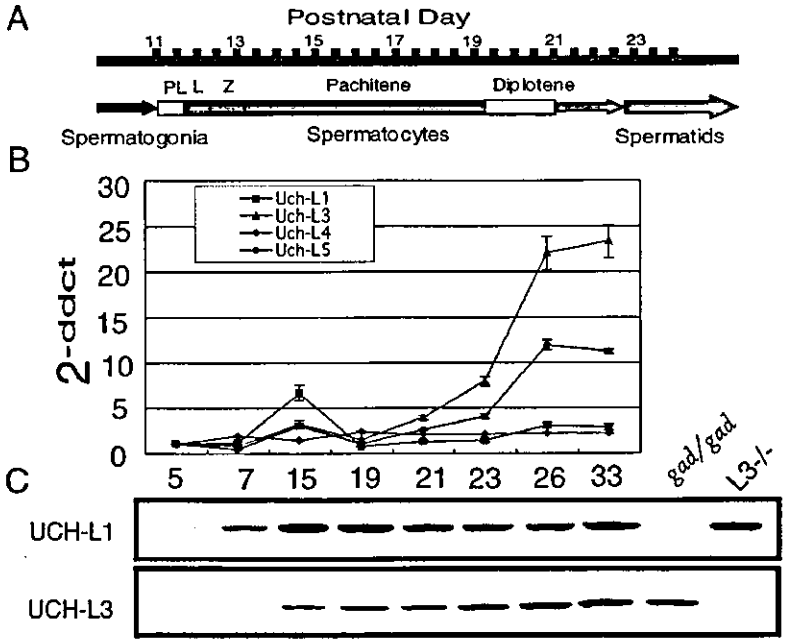

FIG. 5. Expression of UCH isozymes during testicular maturation. A) Timetable for juvenile spermatogenesis. PL, Preleptotene spermatocyte; L, leptotene spermatocyte; Z, zygotene spermatocyte. B) Comparison of the relative UCH isozyme gene expression levels (2^{-ddCt}) by SYBR Green-based real-time quantitative RT-PCR. The value for gene expression from the testes of 5-day-old mice was set to 1.0. C) Comparison of UCH-L1 and UCH-L3 expression by Western blotting. Each lane represents the testes of 5-, 7-, 15-, 19-, 21-, 23-, 26-, or 33-day-old Balb/c mice, *gad* mice, and *Uchl3* knockout mice ($L3^{-/-}$) (B, C).

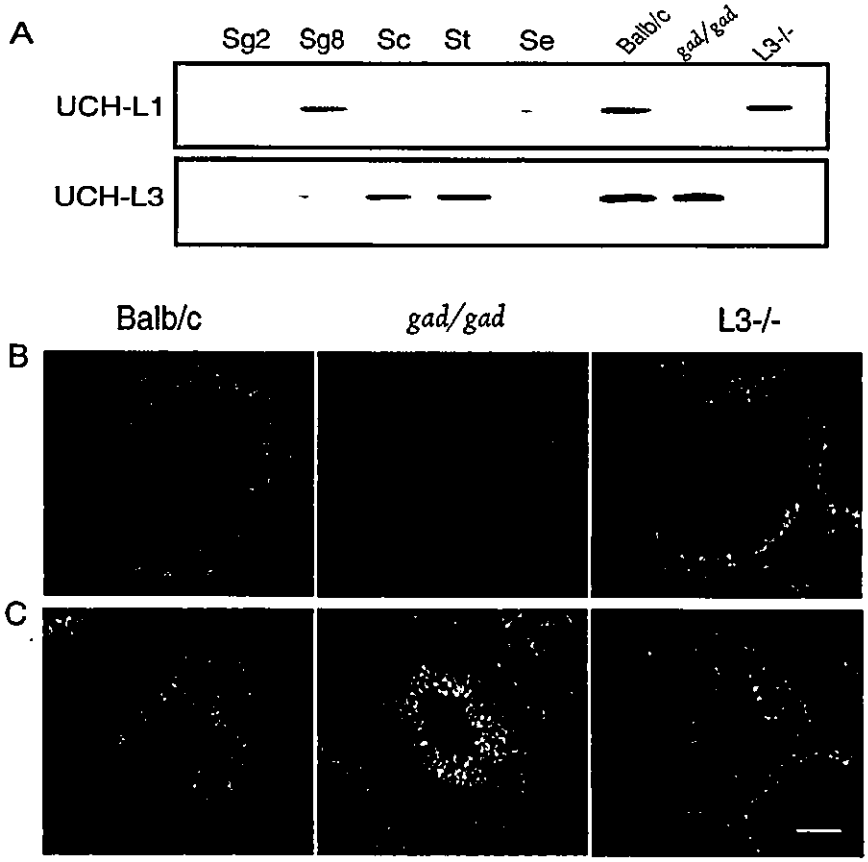

FIG. 6. Analysis of UCH-L1and UCH-L3 expression by western blotting and immunostaining. A) UCH-L1 and UCH-L3 expression in isolated germ cells and Sertoli cells. Sg2, Spermatogonia from 2-wk-old mice; Sg8, spermatogonia from 8-wk-old mice; Sc, spermatocytes from 8-wk-old mice; St, spermatids from 8-wk-old mice; Se, Sertoli cells from 2-wk-old mice. Balb/c, testis from a Balb/c mouse; *gad/gad*, testis from a *gad* mouse (*Uchl1* knockout mouse); $L3^{-/-}$, testis from a *Uchl3* knockout mouse. Immunohistochemistry of UCH-L1 (B) and UCH-L3 (C) in the testis of wild type, *gad*, and *Uchl3* knockout mouse. Stages V–VIII of seminiferous epithelium predominate in each panel as visualized by PAS staining of serial sections. Green fluorescence represents UCH-L1 (B) and UCH-L3 (C); red fluorescence represents staining of cell nuclei by propidium iodide (PI). Magnification, ×200. Scale bar = 30 μm.

clonal antibodies that specifically react with mouse UCH-L3. Using RT-PCR and western blotting, we detected high levels of UCH-L3 mRNA and protein in meiotic pachytene spermatocytes and postmeiotic spermatids during spermatogenesis (Figs. 4B and 6A). These results suggest that UCH-L1 and UCH-L3 may play distinct roles in spermatogenesis, in that UCH-L1 may function in mitotic proliferation, whereas UCH-L3 may function in the meiotic differentiation of spermatocytes into spermatids.

Around Postnatal Day 15, the higher expression of UCH-L1 mRNA suggests that UCH-L1 might have certain functions during testicular maturation. Furthermore, the increased expression of UCH-L1 after Postnatal Day 15 suggests that it might play an active role in mitotic proliferation. In addition to the *Uchl1* genes, we also analyzed transcription from two other UCH isozyme genes, *Uchl3* and *Uchl5*, in isolated testicular cells. UCH-L3 and UCH-L5 mRNAs were found in meiotic pachytene spermatocytes and postmeiotic spermatids (Fig. 4, B and D) and showed similar expression patterns during the course of testicular maturation (Fig. 5B). These results suggest that the *Uchl3* and *Uchl5* genes may have overlapping functions during spermatogenesis. The ubiquitin pathway is very active during the postmitotic phase of spermatogenesis [3, 36]. Thus, UCH-L3 may function to regulate the cell cycle and chromatin structure during the meiotic phase but may facilitate the en masse degradation of cytoplasmic proteins as well as organelle/nuclear remolding during the postmeiotic phase. The present study demonstrates for the first time that UCH-L3 is expressed mainly in meiotic spermatocytes and postmeiotic spermatids during spermatogenesis. Although UCH-L3 shares considerable sequence homology with UCH-L1, the hydrolytic activity of UCH-L3 in vitro differs substantially from that of UCH-L1. The rate of UCH-L3-mediated catalysis (K_{cat}) is more than 200 times greater than UCH-L1 using ubiquitin amide as a substrate [46]. This relatively high activity of UCH-L3 is consistent with its expression during the postmitotic phase of spermatogenesis, in that maturation from spermatocytes to spermatids may be critically dependent on the ubiquitin pathway despite the fact that *Uchl3* knockout mice exhibit normal fertility [13].

In conclusion, our results demonstrate that the expression of UCH isozymes is differentially and developmentally regulated during spermatogenesis and that UCH-L1 and UCH-L3 likely have distinct functions during different developmental phases. These results enhance our understanding of how the ubiquitin pathway is regulated by UCH isozymes during spermatogenesis. Moreover, isolation of mouse germ cells and Sertoli cells from testes may afford the opportunity to assess UCH isozyme function during spermatogenesis in vitro. UCH-L1 has been suggested to associate with monoubiquitin and thereby increase the half-life of ubiquitin in neurons [47]. In addition, a UCH-L1 ubiquityl ligase-like activity has also been proposed [46]. Further biochemical and genetic analyses of UCH family members will help elucidate the role of UCHs in the complex molecular mechanisms involved in spermatogenesis.

REFERENCES

1. Weissman AM. Themes and variations on ubiquitylation. Nat Rev Mol Cell Biol 2001; 2:169–178.
2. Baarends WM, Roest HP, Grootegoed JA. The ubiquitin system in gametogenesis. Mol Cell Endocrinol 1999; 151:5–16.
3. Baarends WM, van der Laan R, Grootegoed JA. Specific aspects of the ubiquitin system in spermatogenesis. J Endocrinol Invest 2000; 23:597–604.
4. Ciechanover A, Orian A, Schwartz AL. Ubiquitin-mediated proteolysis: biological regulation via destruction. Bioessays 2000; 22:442–451.
5. Varshavsky A. The ubiquitin system. Trends Biochem Sci 1997; 22: 383–387.
6. Wilkinson KD. Roles of ubiquitinylation in proteolysis and cellular regulation. Annu Rev Nutr 1995; 15:161–189.
7. Grimes SR, Wilkerson DC, Noss KR, Wolfe SA. Transcriptional control of the testis-specific histone H1t gene. Gene 2003; 304:13–21.
8. Wilkinson KD. Regulation of ubiquitin-dependent processes by deubiquitinating enzymes. FASEB J 1997; 11:1245–1256.
9. Mayer AN, Wilkinson KD. Detection, resolution, and nomenclature of multiple ubiquitin carboxyl-terminal esterases from bovine calf thymus. Biochemistry 1989; 28:166–172.
10. Kurihara LJ, Kikuchi T, Wada K, Tilghman SM. Loss of Uch-L1 and Uch-L3 leads to neurodegeneration, posterior paralysis and dysphagia. Hum Mol Genet 2001; 10:1963–1970.
11. Saigoh K, Wang YL, Suh JG, Yamanishi T, Sakai Y, Kiyosawa H, Harada T, Ichihara N, Wakana S, Kikuchi T, Wada K. Intragenic deletion in the gene encoding ubiquitin carboxy-terminal hydrolase in gad mice. Nat Genet 1999; 23:47–51.
12. Wilkinson KD, Deshpande S, Larsen CN. Comparisons of neuronal (PGP 9.5) and non-neuronal ubiquitin C-terminal hydrolases. Biochem Soc Trans 1992; 20:631–637.
13. Kurihara LJ, Semenova E, Levorse JM, Tilghman SM. Expression and functional analysis of Uch-L3 during mouse development. Mol Cell Biol 2000; 20:2498–2504.
14. Zhang N, Wilkinson K, Bownes M. Cloning and analysis of expression of a ubiquitin carboxyl terminal hydrolase expressed during oogenesis in *Drosophila melanogaster*. Dev Biol 1993; 157:214–223.
15. Wilson PO, Barber PC, Hamid QA, Power BF, Dhillon AP, Rode J, Day IN, Thompson RJ, Polak JM. The immunolocalization of protein gene product 9.5 using rabbit polyclonal and mouse monoclonal antibodies. Br J Exp Pathol 1988; 69:91–104.
16. Tokunaga Y, Imai S, Torii R, Maeda T. Cytoplasmic liberation of protein gene product 9.5 during the seasonal regulation of spermatogenesis in the monkey (*Macaca fuscata*). Endocrinology 1999; 140: 1875–1883.
17. Kon Y, Endoh D, Iwanaga T. Expression of protein gene product 9.5, a neuronal ubiquitin C-terminal hydrolase, and its developing change in Sertoli cells of mouse testis. Mol Reprod Dev 1999; 54:333–341.
18. Kwon J, Kikuchi T, Setsuie R, Ishii Y, Kyuwa S, Yoshikawa Y. Characterization of the testis in congenitally ubiquitin carboxy-terminal hydrolase-1 (Uch-L1) defective (gad) mice. Exp Anim 2003; 52:1–9.
19. Loveland KL, Schlatt S. Stem cell factor and c-kit in the mammalian testis: lessons originating from mother nature's gene knockouts. J Endocrinol 1997; 153:337–344.
20. Lassalle B, Ziyyat A, Testart J, Finaz C, Lefevre A. Flow cytometric method to isolate round spermatids from mouse testis. Hum Reprod 1999; 14:388–394.
21. van der Wee KS, Johnson EW, Dirami G, Dym TM, Hofmann MC. Immunomagnetic isolation and long-term culture of mouse type A spermatogonia. J Androl 2001; 22:696–704.
22. van Pelt AM, Morena AR, van Dissel-Emiliani FM, Boitani C, Gaemers IC, de Rooij DG, Stefanini M. Isolation of the synchronized A spermatogonia from adult vitamin A-deficient rat testes. Biol Reprod 1996; 55:439–444.
23. von Schonfeldt V, Krishnamurthy H, Foppiani L, Schlatt S. Magnetic cell sorting is a fast and effective method of enriching viable spermatogonia from Djungarian hamster, mouse, and marmoset monkey testes. Biol Reprod 1999; 61:582–589.
24. Kato S, Kobayashi T, Kusuda K, Nishina Y, Nishimune Y, Yomogida K, Yamamoto M, Sakagami H, Kondo H, Ohnishi M, Chida N, Yanagawa Y, Tamura S. Differentiation-dependent enhanced expression of protein phosphatase 2Cbeta in germ cells of mouse seminiferous tubules. FEBS Lett 1996; 396:293–297.
25. Anthony CT, Skinner MK. Cytochemical and biochemical characterization of testicular peritubular myoid cells. Biol Reprod 1989; 40: 811–823.
26. Scarpino S, Morena AR, Petersen C, Froysa B, Soder O, Boitani C. A rapid method of Sertoli cell isolation by DSA lectin, allowing mitotic analyses. Mol Cell Endocrinol 1998; 146:121–127.
27. Cox WG, Singer VL. A high-resolution, fluorescence-based method for localization of endogenous alkaline phosphatase activity. J Histochem Cytochem 1999; 47:1443–1456.

28. Bellve AR. Purification, culture, and fractionation of spermatogenic cells. Methods Enzymol 1993; 225:84–113.
29. Malkov M, Fisher Y, Don J. Developmental schedule of the postnatal rat testis determined by flow cytometry. Biol Reprod 1998; 59:84–92.
30. Sorrentino V, Giorgi M, Geremia R, Besmer P, Rossi P. Expression of the c-kit proto-oncogene in the murine male germ cells. Oncogene 1991; 6:149–151.
31. Kurth BE, Wright RM, Flickinger CJ, Herr JC. Stage-specific detection of mRNA for the sperm antigen SP-10 in human testes. Anat Rec 1993; 236:619–625.
32. Mauduit C, Hamamah S, Benahmed M. Stem cell factor/c-kit system in spermatogenesis. Hum Reprod Update 1999; 5:535–545.
33. Aoki K, Sun YJ, Aoki S, Wada K, Wada E. Cloning, expression, and mapping of a gene that is upregulated in adipose tissue of mice deficient in bombesin receptor subtype-3. Biochem Biophys Res Commun 2002; 290:1282–1288.
34. Janca FC, Jost LK, Evenson DP. Mouse testicular and sperm cell development characterized from birth to adulthood by dual parameter flow cytometry. Biol Reprod 1986; 34:613–623.
35. Aoki S, Su Q, Li H, Nishikawa K, Ayukawa K, Hara Y, Namikawa K, Kiryu-Seo S, Kiyama H, Wada K. Identification of an axotomy-induced glycosylated protein, AIGP1, possibly involved in cell death triggered by endoplasmic reticulum-Golgi stress. J Neurosci 2002; 22: 10751–10760.
36. Sutovsky P. Ubiquitin-dependent proteolysis in mammalian spermatogenesis, fertilization, and sperm quality control: killing three birds with one stone. Microsc Res Tech 2003; 61:88–102.
37. Wing SS. Deubiquitinating enzymes—the importance of driving in reverse along the ubiquitin-proteasome pathway. Int J Biochem Cell Biol 2003; 35:590–605.
38. Guardavaccaro D, Kudo Y, Boulaire J, Barchi M, Busino L, Donzelli M, Margottin-Goguet F, Jackson PK, Yamasaki L, Pagano M. Control of meiotic and mitotic progression by the F box protein beta-Trcp1 in vivo. Dev Cell 2003; 4:799–812.
39. van Baren MJ, van der Linde HC, Breedveld GJ, Baarends WM, Rizzu P, de Graaff E, Oostra BA, Heutink P. A double RING-H2 domain in RNF32, a gene expressed during sperm formation. Biochem Biophys Res Commun 2002; 292:58–65.
40. Escalier D, Bai XY, Silvius D, Xu PX, Xu X. Spermatid nuclear and sperm periaxonemal anomalies in the mouse Ube2b null mutant. Mol Reprod Dev 2003; 65:298–308.
41. Baarends WM, Wassenaar E, Hoogerbrugge JW, van Cappellen G, Roest HP, Vreeburg J, Ooms M, Hoeijmakers JH, Grootegoed JA. Loss of HR6B ubiquitin-conjugating activity results in damaged synaptonemal complex structure and increased crossing-over frequency during the male meiotic prophase. Mol Cell Biol 2003; 23:1151–1162.
42. Roest HP, van Klaveren J, de Wit J, van Gurp CG, Koken MH, Vermey M, van Roijen JH, Hoogerbrugge JW, Vreeburg JT, Baarends WM, Bootsma D, Grootegoed JA, Hoeijmakers JH. Inactivation of the HR6B ubiquitin-conjugating DNA repair enzyme in mice causes male sterility associated with chromatin modification. Cell 1996; 86: 799–810.
43. Escalier D. New insights into the assembly of the periaxonemal structures in mammalian spermatozoa. Biol Reprod 2003; 69:373–378.
44. Hershko A, Ciechanover A. The ubiquitin system for protein degradation. Annu Rev Biochem 1992; 61:761–807.
45. Osawa Y, Wang YL, Osaka H, Aoki S, Wada K. Cloning, expression, and mapping of a mouse gene, Uchl4, highly homologous to human and mouse Uchl3. Biochem Biophys Res Commun 2001; 283:627–633.
46. Liu Y, Fallon L, Lashuel HA, Liu Z, Lansbury PT Jr. The UCH-L1 gene encodes two opposing enzymatic activities that affect alpha-synuclein degradation and Parkinson's disease susceptibility. Cell 2002; 111:209–218.
47. Osaka H, Wang YL, Takada K, Takizawa S, Setsuie R, Li H, Sato Y, Nishikawa K, Sun YJ, Sakurai M, Harada T, Hara Y, Kimura I, Chiba S, Namikawa K, Kiyama H, Noda M, Aoki S, Wada K. Ubiquitin carboxy-terminal hydrolase L1 binds to and stabilizes monoubiquitin in neuron. Hum Mol Genet 2003; 12:1945–1958.